Acta Med. Okayama, 2009
Vol. 63, No. 2, pp. 87–96

Acta Medica Okayama
http://escholarship.lib.okayama-u.ac.jp/amo/

Original Article

Doppler Echocardiographic Assessment of Left Ventricular Diastolic Function in Chronic Hypoxic Rats

Atsushi Itoh[a], Hideshi Tomita[b], and Shunji Sano[a]*

[a]*Department of Cardiovascular Surgery, Okayama University Graduate School of Medicine, Dentistry and Pharmaceutical Sciences, Okayama 700–8558, Japan, and*
[b]*Department of Cardiovascular Center, Showa University Northern Yokohama Hospital, Yokohama 224–8503, Japan*

Little information is available on the mechanism of diastolic left ventricular (LV) dysfunction in patients with chronic respiratory disease complicated by hypoxia. The purpose of this study was to investigate how chronic hypoxia impairs LV diastolic function in an hypoxic animal model. Thirty-six male Wistar rats 8 weeks old were assigned to normoxia (N), chronic hypoxia (CH), and re-normoxia (RN) groups, 12 rats per group. The N group rats were kept in ambient air for 8 weeks, while the CH group was kept hypoxic for 8 weeks. After 8 weeks of hypoxia the RN group rats were kept for a further 8 weeks in ambient air. LV systolic and diastolic functions, as well as right ventricular (RV) function, were analyzed using Doppler echocardiography; we also measured the hematocrit, and weighed the LV and RV. Hematocrit, RV weight/body weight, and RV weight/LV weight were higher in the CH group than in the other 2 groups. However, most of these parameters returned to normoxia levels after re-normoxia. In the CH group, LV dimension and area were smaller than in the other 2 groups. LV systolic function was preserved in all groups; however, in the CH group, mitral flow showed a restrictive pattern, while pulmonary flow demonstrated a pulmonary hypertensive pattern with prolonged RV ejection time. In conclusion, chronic hypoxia induced pulmonary hypertension and RV hypertrophy. Although LV systolic function was preserved, diastolic function was impaired in hypoxia. Ventricular interaction may impair LV diastolic function.

Key words: chronic hypoxia, left ventricular diastolic function, pulmonary hypertension, right ventricular hypertrophy, ventricular interaction

Left ventricular (LV) diastolic dysfunction occasionally complicates chronic respiratory disease associated with hypoxia, such as chronic obstructive pulmonary disease (COPD) [1, 2], pulmonary arterial hypertension [3–6], obstructive sleep apnea [7], chronic thromboembolic pulmonary hypertension (CTEPH) [8–10], and systemic sclerosis [11]. Right ventricular (RV) dilatation and/or RV hypertrophy, resulting from pulmonary hypertension (PH) secondary to hypoxic pulmonary vasoconstriction [12], may distort the LV and impair its function. This ventricular interaction has been well described [13] and been shown to result in impaired LV diastolic function.

However, in actual clinical situations, such chronic respiratory disease is prevalent in the elderly, and

Received October 17, 2008; accepted December 4, 2008.
*Corresponding author. Phone:+81–86–235–7357; Fax:+81–86–235–7541
E-mail:s_sano@cc.okayama-u.ac.jp (S. Sano)

often co-exists with systemic hypertension and/or coronary artery disease which may also impair LV function. Consequently, it is occasionally difficult to determine the major culprit in patients with LV dysfunction.

The purpose of this study was to investigate the hemodynamic effects of chronic hypoxia particularly on LV diastolic function using Doppler echocardiography in an animal model—the chronic hypoxic rat developed by Nakanishi *et al.* in our laboratory [14]. This model has important advantages in that no surgical manipulation is required, and a uniform model can be created easily and reliably. With this model, we can analyze the hemodynamic effects of chronic hypoxia isolated from other influencing factors. We used Doppler echocardiography to evaluate anatomical and hemodynamic changes following chronic hypoxia. Doppler echocardiography is a well established means of analyzing not only LV systolic [15] but also diastolic function [16–18], while a few parameters of RV function can be derived from pulmonary blood flow patterns [19]. Furthermore, we believe it is an optimum approach to assessing ventricular interaction in the beating heart.

Materials and Methods

Animals. Thirty-six male 8-week-old Wistar rats (Charles River Japan Inc., Yokohama, Japan) weighing 280 to 300 g were used. They were treated in compliance with the "Guidelines for Animal Experiments at Okayama University Medical School" (our institutional guidelines and approval).

Experimental groups. The rats were randomly allocated to one of 3 groups: normoxia (control, N), chronic hypoxia (CH), and re-normoxia (RN), 12 rats per group. The CH group was housed in a normobaric hypoxic chamber for 8 weeks, the N group was housed in ambient air for the same period, and the RN group was kept in the hypoxic chamber for 8 weeks, and subsequently housed in ambient air for another 8 weeks.

Chronic hypoxic rat model. Rats were kept in hypoxic conditions as previously described by our laboratory [14]. Briefly, the environment within the hypoxic chamber was continuously monitored with an oxygen analyzer and its oxygen concentration was maintained within $10 \pm 0.1\%$. Chamber air was analyzed periodically, and the inspired carbon dioxide fraction within the chamber was maintained at less than 0.4% at all times. Humidity within the hypoxic chamber was maintained at less than 70%, and the temperature was kept between 22 and 26°C. All the N, CH and RN rats were kept in the same room under the same light-dark cycle. Rat chow and tap water were provided ad libitum. CH rats did not demonstrate any respiratory difficulties while in the hypoxic chamber.

Echocardiography. After the hypoxic or normoxic exposure period, all rats were weighed and underwent transthoracic Doppler echocardiography in a hypoxic or normoxic environment. Previous reports have confirmed the accuracy and reproducibility of this technique for measuring cardiac function in rats [15–19]. We used this method for our study with some modifications. Briefly, rats were anesthetized with ketamine HCl (50 mg/kg; Sankyo Lifetech Co., Ltd., Tokyo, Japan) and xylazine (10 mg/kg; Bayer Medical Ltd., Tokyo, Japan), both given intraperitoneally. Rats were allowed to breathe spontaneously during the echocardiography. The rat's chest was shaved, and rats were placed in the supine or lateral decubitus position on a warming table. An ECG was obtained with standard limb electrodes and the heart rate was monitored continuously. After a layer of acoustic coupling gel was applied to the thorax, two-dimensional and M-mode echocardiograms with Doppler were obtained using a commercially available fully digital ALOKA ProSound II SSD6500 ultrasonographic system (ALOKA Co., Tokyo, Japan), with a 13-MHz linear array transducer (UST-5545). The system software was modified to allow for 230-Hz maximal frame rate recordings with an area of interest <30 mm from the surface of the transducer; changes specifically designed for cardiac ultrasonic studies in rats. The high-frequency transducer used in this study ensured good transthoracic images of the beating heart. Images were obtained by placing the transducer directly on the left anterior side of the chest, and care was taken to avoid excessive pressure on the thorax, which can induce severe bradycardia. The transducer was maximally aligned to optimize endocardial visualization and spectral displays of Doppler profiles. All recordings were digitally transferred to an on-line computer and captured by eDMS (data analysis system built-in to the US machine) for

subsequent analysis. The heart was first imaged in two-dimensional mode using parasternal short-axis views of the left ventricle; once the papillary muscle was well visualized, the two-dimensional and M-mode images were recorded. In the two-dimensional mode, measurements on the left ventricular short-axis endocardial area tracings were performed on-line at end-diastole (the time of apparent maximal cavity dimension) and end-systole (the time of maximum anterior motion of the posterior wall) phase using the cine-loop feature to obtain adequate visualization of the fast-beating hearts, retrospectively. The tracings were analyzed by a single experienced technical sonographer (T.Y.) who had no knowledge of the study group. M-mode tracings were recorded at the same level, and anterior and posterior wall thicknesses as well as LV internal dimensions were measured. End-diastolic and end-systolic LV internal diameters were measured by the leading-edge method to determine the maximal LV end-diastolic dimension (LVDd) and minimal LV end-systolic dimension (LVDs) according to the American Society of Echocardiography. As the leading edge of the anterior wall is often difficult to identify, the inner edge of this wall was used. LV ejection time was measured as the time from end diastole to end systole. All measurements were made in a blinded manner and averaged over 5 consecutive cardiac cycles, and were made to a precision of 0.1 mm. Global left ventricular systolic function was assessed by calculating the fractional shortening (FS), mean velocity of circumferential fiber shortening (mVcf), and fractional area change (FAC).

The FS (%) was calculated as [(LVDd-LVDs)/LVDd] × 100,
where LVDd is the LV internal end-diastolic dimension and LVDs is the LV internal end-systolic dimension.

The mVcf was calculated as FS/LVET,
where LVET is the LV ejection time.

The FAC (%) was calculated as [(LVDa-LVSa)/LVDa] × 100,
where LVDa is the LV end-diastolic area and LVSa is the LV end-systolic area.

To correct for differences in body and heart size in N, CH and RN groups, data for each rat were normalized by tibial length (TL). Variables expressed as ratios, such as FS, mVcf and FAC, were not normalized. To assess left ventricular diastolic function, two-dimensionally guided pulsed-wave Doppler spectra of mitral inflow were recorded from an apical four-chamber view, with the sample volume placed near the tips of the mitral leaflets and positioned where velocity was maximal and the flow pattern was laminar (Fig. 1A). The sample volume was adjusted to the smallest size available (0.5 mm). Measurements represent the means of at least 5 consecutive cardiac cycles, and include peak early filling velocity (E velocity), late filling velocity (A velocity), their ratio (E/A), and the deceleration slope of the early filling wave (E Deceleration). To assess RV function, pulse Doppler of the pulmonary outflow was recorded from the parasternal view at the level of the aortic valve (Fig. 1B). The sample volume was placed proximal to the pulmonary valve leaflets and aligned to maximize laminar flow. In

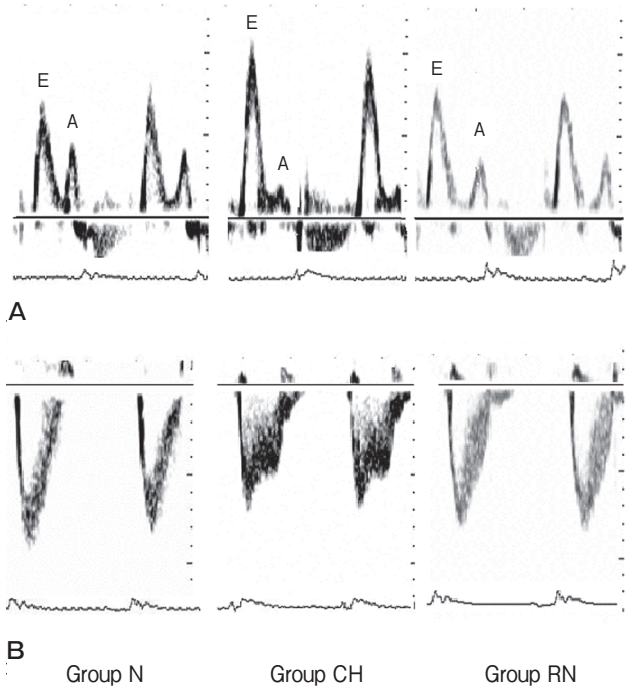

Fig. 1 **A**, Example of pulse Doppler mitral inflow pattern in the normoxic/control rat (left), the chronic hypoxic rat (middle), and the re-normoxic rat (right). Compared with the normoxic/control rat, the mitral inflow pattern in the chronic hypoxic rat shows increased E velocity, rapid deceleration of E wave, and decreased A velocity; **B**, Example of pulse Doppler pulmonary blood pattern in the normoxic/control rat (left), in the chronic hypoxic rat (middle), and in the re-normoxic rat (right). Compared with the normoxic/control rat, the pulmonary blood pattern from the chronic hypoxic rat shows decreased peak flow velocity, rapid AT, and prolonged RVET. Note the early notching in the chronic hypoxic rat (mid-systolic dip pattern).

addition to characterizing the pulmonary outflow Doppler envelope, the acceleration time (AT), peak pulmonary outflow velocity (Peak velocity), and RV ejection time (RVET) were measured. Acceleration time was measured from the onset of systolic flow to peak pulmonary outflow velocity. RV ejection time was measured from the onset of systolic pulmonary flow to its completion.

Evaluation of hypoxia. Peripheral oxygen saturation was determined using the tail cuff method (Tycohealthcare N550) during echocardiography. Blood samples to measure the hematocrit (Hct), as a marker of polycythemia following chronic hypoxia, were collected after echocardiography also in a hypoxic or normoxic environment. Duplicate hematocrit samples were prepared in microhematocrit tubes and Hct was determined.

Wet body weight (BW). After the echocardiographic study, the rats were killed by injecting an overdose of ketamine and xylazine. The thorax was opened, the heart was removed and the atria and great vessels were dissected free. The RV free wall and LV wall (LV free wall + ventricular septum) were weighed separately. The ratios of RV wall (milligrams)/BW (grams) and RV/LV were calculated. In the chronic hypoxic rats the tissues were excised in a hypoxic environment.

Tibial length (TL). At the end of the experiment, the rats' right hind legs were removed by disarticulating the femur from the acetabulum at the hip. Radiographic films of the tibias were then obtained, and the TL of each rat was measured from the radiograph with calipers.

Statistical analysis. All data are expressed as means ± standard deviations. Parameters among groups were compared with a one way analysis of variance without replication. The post-hoc test employed Fisher's protected least significant difference (PLSD) test using StatView 5.0 software (SAS Institute, Cary, NC, USA). A p value less than 0.05 was regarded as statistically significant.

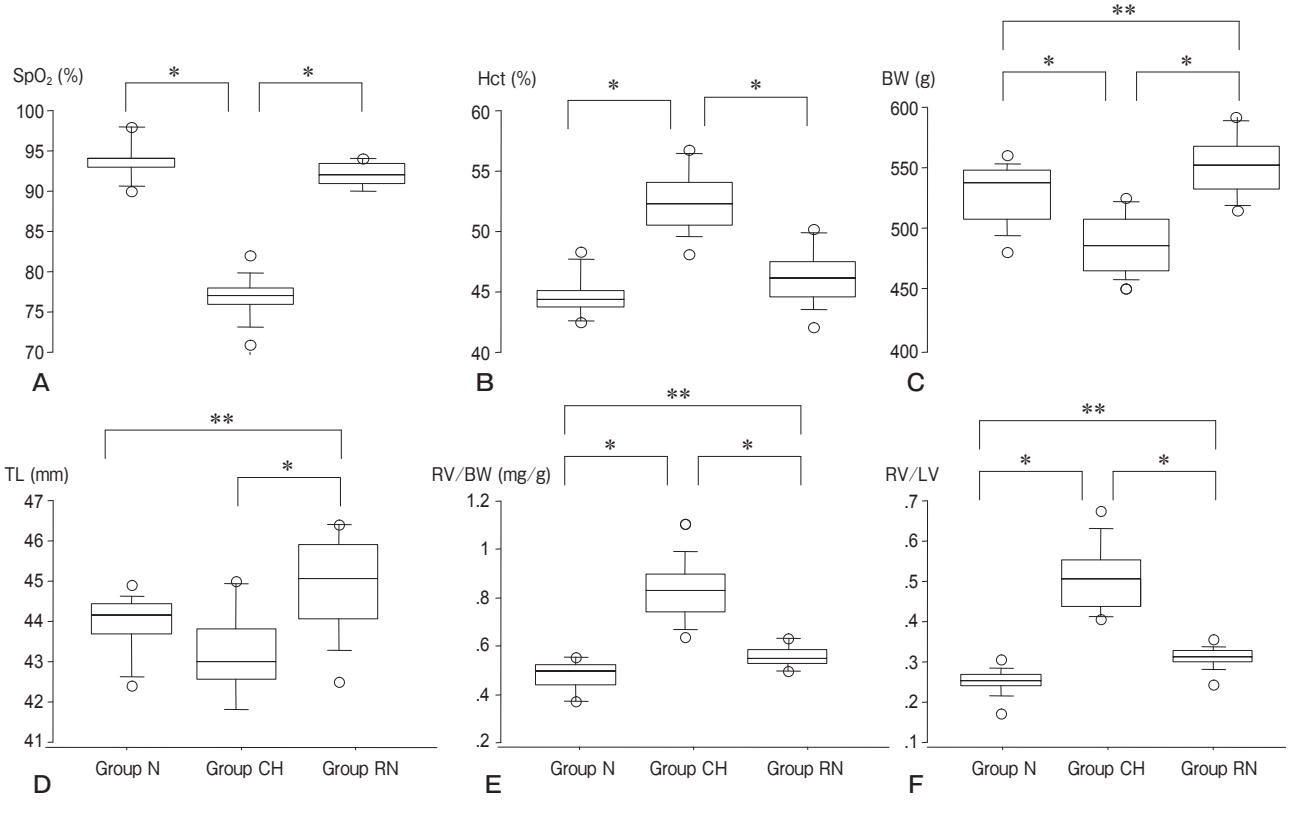

Fig. 2 SpO_2 (A), Hct (B), BW (C), TL (D), RV/BW (E), and RV/LV (F) in each group. The bar of each column in figure shows, from bottom to top, the 10th, 25th, 50th, 75th, and 90th percentile of each group. * and ** in figure indicate p value of <0.01 and <0.05 by the post-hoc test (Fisher's PLSD), respectively.

Table 1 Demographic characteristics, laboratory data and Doppler echocardiographic data

	Group N (n=12)		Group CH (n=12)		Group RN (n=12)		*p*
Demographic characteristics							
Age (weeks old)	16		16		24		
SpO_2 (%)*	94±2	(90–98)	77±2	(71–82)	92±1	(90–94)	<0.01
HR (beats/min)*	243±15	(216–270)	248±20	(221–297)	246±20	(219–279)	ns
Hct (%)	44±1	(43–48)	52±2	(48–56)	46±2	(42–50)	<0.01
BW (g)	528±25	(480–560)	487±24	(460–525)	553±25	(515–595)	<0.01
TL (mm)	44.0±0.7	(42.4–44.9)	43.1±1.0	(41.8–45.0)	44.8±1.1	(42.5–46.4)	<0.01
RV/BW (mg/g)	0.47±0.06	(0.37–0.55)	0.82±0.12	(0.64–1.10)	0.55±0.04	(0.50–0.63)	<0.01
RV/LV	0.25±0.03	(0.17–0.30)	0.50±0.08	(0.41–0.67)	0.31±0.02	(0.24–0.35)	<0.01
Left ventricular geometry							
LVDd/TL (cm/m)	20.0±0.8	(18.8–21.6)	17.3±0.7	(16.0–18.1)	19.7±0.9	(18.3–20.7)	<0.01
LVDa/TL (cm^2/m)	15.0±1.4	(12.9–17.9)	12.7±0.6	(11.6–13.5)	14.7±1.4	(13.1–17.8)	<0.01
Left ventricular systolic function							
FS (%)	40±3	(35–45)	40±3	(35–44)	43±4	(38–52)	<0.05
mVcf (circ/sec)	4.0±0.3	(3.5–4.1)	3.9±0.2	(3.4–4.1)	4.3±0.4	(3.5–4.9)	<0.05
FAC (%)	61±3	(54–67)	64±3	(58–68)	52±4	(45–58)	<0.01
Left ventricular diastolic function							
E velocity (m/sec)	0.79±0.06	(0.70–0.88)	0.99±0.07	(0.86–1.16)	0.80±0.05	(0.73–0.93)	<0.01
A velocity (m/sec)	0.43±0.04	(0.34–0.49)	0.19±0.01	(0.17–0.22)	0.41±0.05	(0.33–0.54)	<0.01
E/A	1.8±0.1	(1.5–2.0)	5.2±0.2	(4.6–5.5)	2.0±0.3	(1.4–2.8)	<0.01
E Deceleration (m/sec^2)	18±1	(16–20)	29±2	(27–33)	19±3	(15–27)	<0.01
Right ventricular outflow							
Peak velocity (m/sec)	0.86±0.07	(0.72–0.95)	0.73±0.06	(0.60–0.87)	0.85±0.05	(0.79–0.92)	<0.01
RVET (msec)	86±6	(78–99)	104±8	(89–121)	93±7	(82–104)	<0.01
AT (msec)	36±3	(30–41)	24±2	(18–26)	34±3	(26–39)	<0.01
AT/RVET	0.41±0.04	(0.34–0.50)	0.23±0.02	(0.17–0.25)	0.36±0.04	(0.29–0.45)	<0.01

*measured under anesthesia. Values are means ± standard deviation. (range)

N, Normoxia; CH, Chronic hypoxia; RN, Re-normoxia; SpO_2, peripheral oxygen saturation; HR, heart rate; Hct, hematocrit value; BW, body weight; TL, tibial length; RV, right ventricle wet weight; LV, left ventricle wet weight. LVDd, left ventricular internal end-diastolic dimension; LVDa, left ventricular end-diastolic area; TL, tibial length; FS, fractional shortening; mVcf, mean velocity of circumferential fiber shortening; FAC, fractional area change. E velocity, peak early filling velocity; A velocity, late filling velocity; E/A, the ratio of early to late; E Deceleration, the deceleration of slope of the early filling wave. AT, acceleration time; RVET, right ventricular ejection time; *p*, probability value by analysis of variance without replication; ns, not significant.

Results

Demographic and laboratory data. In the CH group, SpO_2 was significantly lower, and the Hct was higher than in the other 2 groups, while there was no significant difference in the heart rate. BW and TL in the RN group were larger than in the other 2 groups, while body weight in the CH group was less than in the N group. RV/BW and RV/LV in the CH group were larger than in the other 2 groups, while in the RN group they were still larger than in the N group. (Table 1, Fig. 2).

LV geometry. Normalized LVDd and LVDa for the CH group were significantly smaller than for the other 2 groups, while there was no significant difference in these parameters between the N and RN groups. (Table 1, Fig. 3).

LV systolic function. FS and mVcf in the RN group were larger than in the other 2 groups, while FAC in the CH group was larger than in the other 2 groups and in the RN group was smaller than in the other 2 groups. However, differences in these parameters, which were regarded as well preserved, were small (Table 1, Fig. 4).

LV diastolic function. Peak velocity of mitral inflow E wave in the CH group was larger, while the A wave was smaller than in the other 2 groups. Consequently, E/A in this group was strikingly larger than in the other 2 groups. E Deceleration was also larger in the CH group than in the other

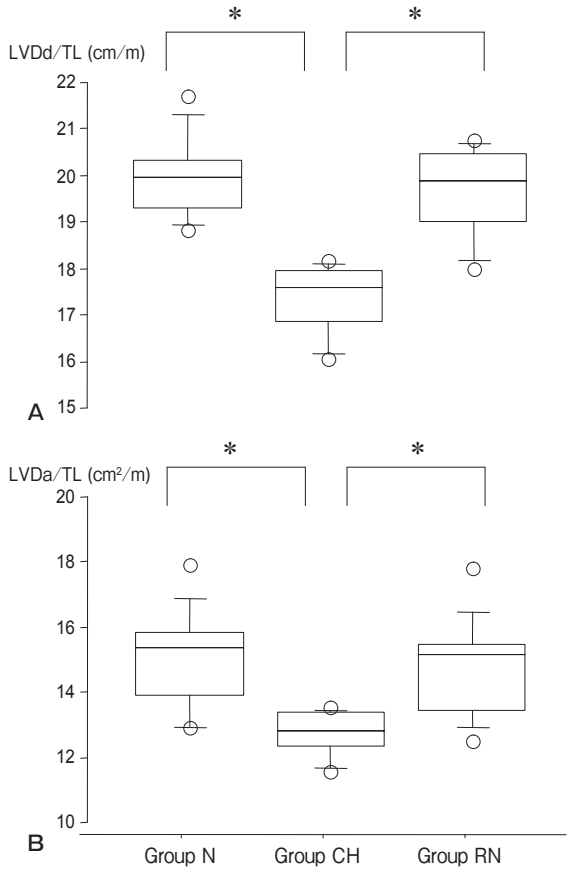

Fig. 3 LVDd/TL (**A**) and LVDa/TL (**B**) in each group. The bar of each column in figure shows, from bottom to top, the 10th, 25th, 50th, 75th, and 90th percentile of each group. * in figure indicates p value of <0.01 by the post-hoc test (Fisher's PLSD).

2 groups (Table 1, Fig. 1A middle, Fig. 5).

Changes of pulmonary blood flow pattern. In the CH group, pulmonary blood flow showed a mid systolic dip pattern, which suggested increased pulmonary vascular resistance (Fig. 1B middle). Peak velocity, AT, and AT/RVET were smaller in the CH group, while RVET was longer than in the other 2 groups. In the RN group, RVET was still longer and AT/RVET was smaller than in the N group (Table 1, Fig. 6).

Discussion

Our main findings in this experiment are summarized as follows. Chronic hypoxic rats developed PH, which led to RV hypertrophy. Although LV systolic function was preserved, the mitral flow pattern showed the so-called restrictive pattern suggesting LV diastolic dysfunction. Such diastolic dysfunction may be caused by functional and anatomical ventricular interaction associated with PH and RV hypertrophy. These changes were almost completely reversed through re-normoxia for 8 weeks, although some effects of hypoxia persisted in several parameters of RV hypertrophy (RV/BW, RV/LV) and PH (RVET and AT/RVET).

How does ventricular interaction impair LV diastolic function? Louie *et al.* reported that the right ventricle continued to contract in the early LV diastole when RVET was prolonged due to PH [3]. Stojnic *et al.* showed that RV pressure exceeded LV pressure in the early diastole in PH following prolongation of RVET [5]. Consequently, the prolonged RVET in PH can impair early LV diastolic filling, and can be described as a phase-dependent ventricular interaction associated with changes in right ventricular ejection characteristics.

The other interaction is anatomic or mechanical, in which a dilated and hypertrophic right ventricle compresses the left ventricle directly or though a shift of the ventricular septum in the limited pericardial space. In our experiment, the left ventricle in chronic hypoxic rats is clearly smaller than in normoxic rats. Furthermore, this may be a reversible process as diastolic function and LV size in the re-normoxic rats were similar to those in normoxic ones. Schena *et al.* reported LV distortion following a shift of the ventricular septum to the LV side [1], while Dittrich *et al.* showed prompt dilatation of LV end diastolic volume following surgical thrombectomy in patients with CTEPH [8].

LV distortion may also have been caused by mechanisms other than mechanical compression, namely, impaired LV preload following decreased RV output associated with PH. The CH group not only had smaller left ventricles but also lower body weight than the N group. As body weight may be partly dependent on cardiac output, the small left ventricle in the CH group could reflect low LV preload. Nootens *et al.* reported that the left ventricle in PH was small [20]. Both compression from the right ventricle and decreased LV preload can distort the LV. From echocardiographic studies before and after thrombectomy in patients with CTEPH, Gurudevan *et al.* concluded that low LV preload was the major

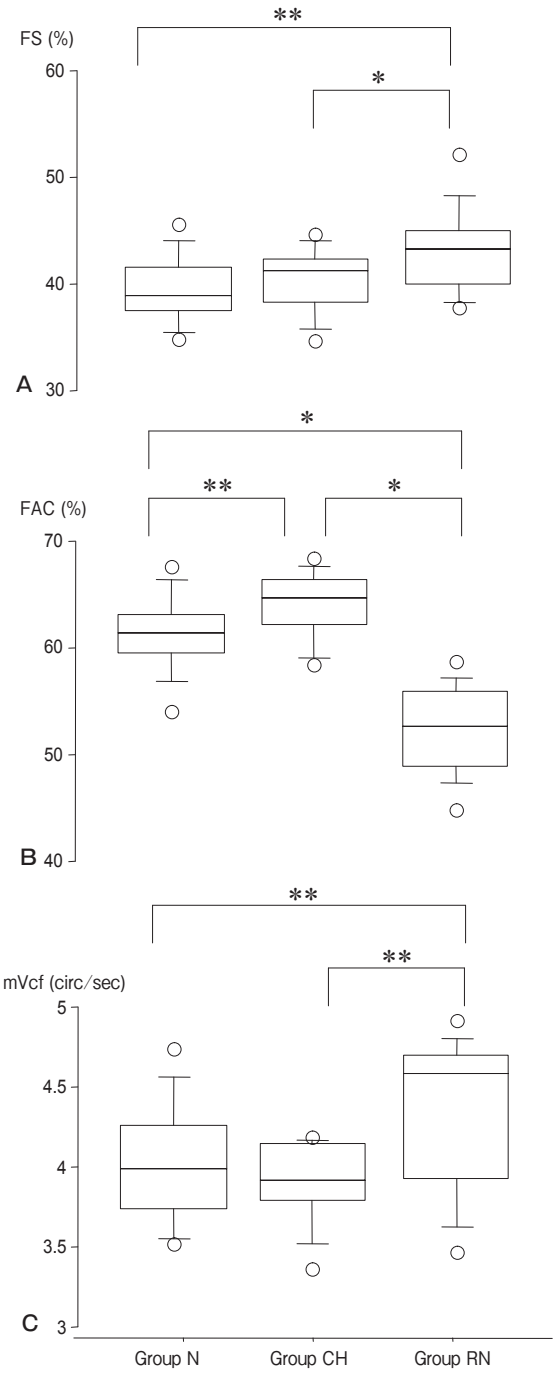

Fig. 4 FS (**A**), FAC (**B**), and mVcf (**C**) in each group. The bar of each column in figure shows, from bottom to top, the 10th, 25th, 50th, 75th, and 90th percentile of each group. * and ** in figure indicate p value of <0.01 and <0.05 by the post-hoc test (Fisher's PLSD), respectively.

determinant of LV distortion [10].

LV myocardial damage during hypoxia might be another cause of LV dysfunction. Although we did not investigate histological changes in the LV myocardium, irreversible changes should be unlikely as LV diastolic function in the re-normoxia group was comparable to that in normoxia. A few studies have reported that hypoxic conditions similar to our experiment did not cause LV myocardial damage [21–23].

Stritzke J *et al.* reported that concentric left ventricular hypertrophy was common in patients with high Hct as a result of an elevated afterload associated with the high viscosity of the blood and increased peripheral resistance [24]. In our experiment, the Hct was elevated in the hypoxic group. We do not have enough data, such as erythropoietin level or a central venous pressure, to document whether the high Hct indicates true polycythemia or is associated with decreased circulating blood volume. However, we believe that it is true polycythemia in response to hypoxia, as there was no significant change in heart rate during hypoxia, which would have been increased in hypovolemia. Future studies will be required to understand whether this high Hct contributes to changes in LV diastolic function.

In our analysis, there were several statistical differences in parameters of LV systolic function, which was preserved in chronic hypoxic rats. Several studies have described findings similar to ours. Louie *et al.* reported preserved LV systolic function in patients with RV pressure overload, while it was impaired in patients with RV volume overload [14, 25]. Noordegraaf *et al.* using MRI, found preserved LV ejection fraction in patients with COPD [26]. However, several investigators have reported abnormalities in the regional wall motion of the ventricular septum, which was compensated for by the other areas. Badke concluded that chronic RV pressure overload was associated with significant changes in LV diastolic shape but maintenance of normal LV systolic function [27]. Goto *et al.* demonstrated that changes in LV geometry during acute RV pressure overload were associated with nonuniform regional changes in systolic shortening in the LV minor axis that were enhanced when the pericardium was intact [28]. Doi *et al.* demonstrated LV dyssynchrony in patients with RV pressure overload [29].

Since echocardiographic functional studies in rats

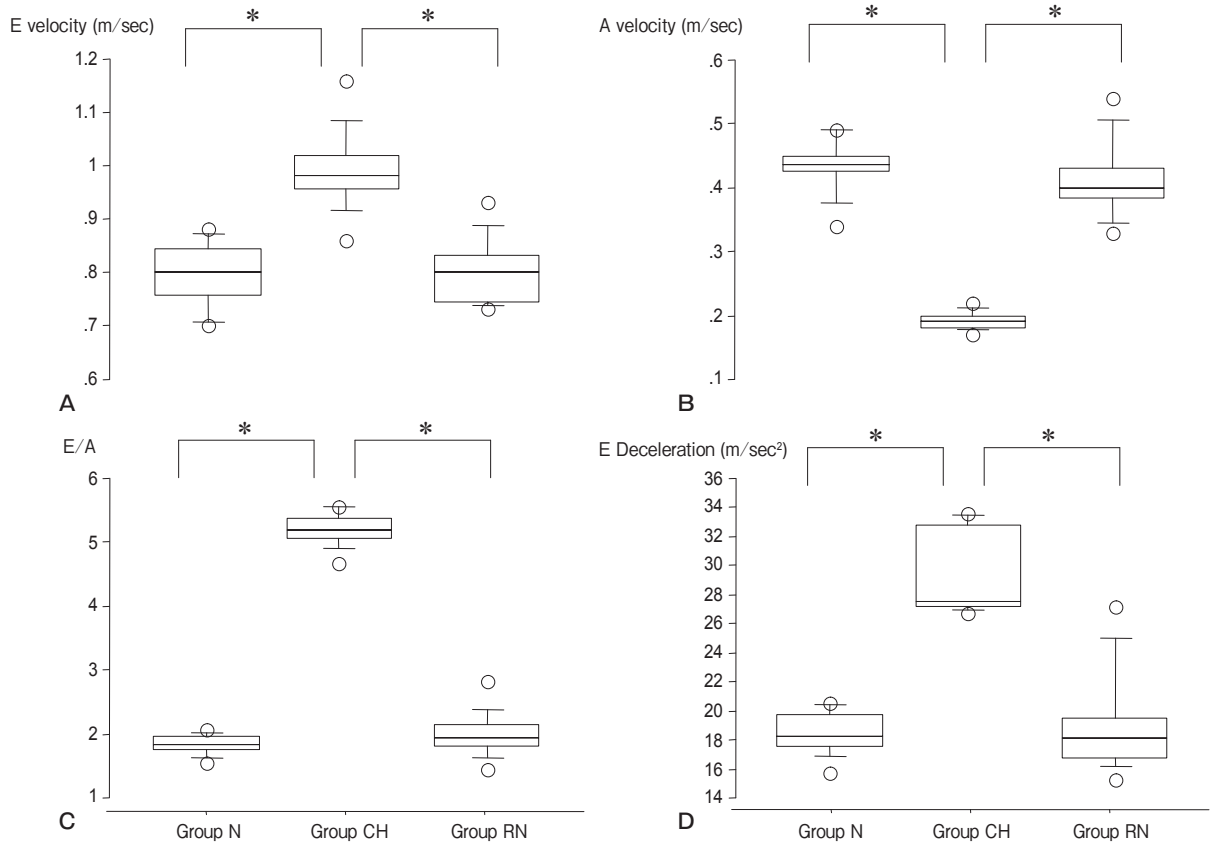

Fig. 5 E velocity (A), A velocity (B), E/A (C), and E Deceleration (D) in each group. The bar of each column in figure shows, from bottom to top, the 10th, 25th, 50th, 75th, and 90th percentile of each group. * in figure indicates p value of <0.01 by the post-hoc test (Fisher's PLSD).

were first reported by Litwin *et al.* [15, 16], it has become possible to analyze LV systolic and diastolic function [17, 18], and pulmonary blood flow pattern as a parameter of RV function [19]. Furthermore, it has become easy to evaluate phase- and time-dependent changes in geometries and blood flow. However, we can not clearly assess tricuspid regurgitation and have therefore been unable to quantify PH. Jones *et al.* reported that tricuspid regurgitation developed when pulmonary artery pressure exceeded 65 mmHg in monocrotaline-induced PH rats [19]. Pulmonary pressure in our chronic hypoxic rats could be lower than that level; meanwhile, the echo probe itself, by compressing various structures, could impede visualization of blood flow close to the body surface.

Several clinical studies have already documented recovery of LV diastolic function following surgery to ameliorate hypoxia in chronic respiratory diseases: for example, thrombectomy for CTEPH [8–10], volume reduction surgery for emphysema [2], and lung transplantation for end stage pulmonary disease [6]. In similar patients, home oxygen therapy, of which the efficacy for hypoxia has already been reported, may correct not only hypoxia but also lead to reversal of LV diastolic dysfunction, which can be a crucial factor in a better prognosis. Similarly, pulmonary vasodilators, such as bosentan or sildenafil, should contribute not only by decreasing pulmonary pressure but by aiding recovery of LV diastolic dysfunction. Further clinical data on this point should be expected.

Study limitations. In our preliminary experiments, the chronic hypoxic rat uniformly developed LV diastolic dysfunction after 8 weeks of hypoxia (unpublished data). As we aimed to investigate the mechanism of this developed LV diastolic dysfunction

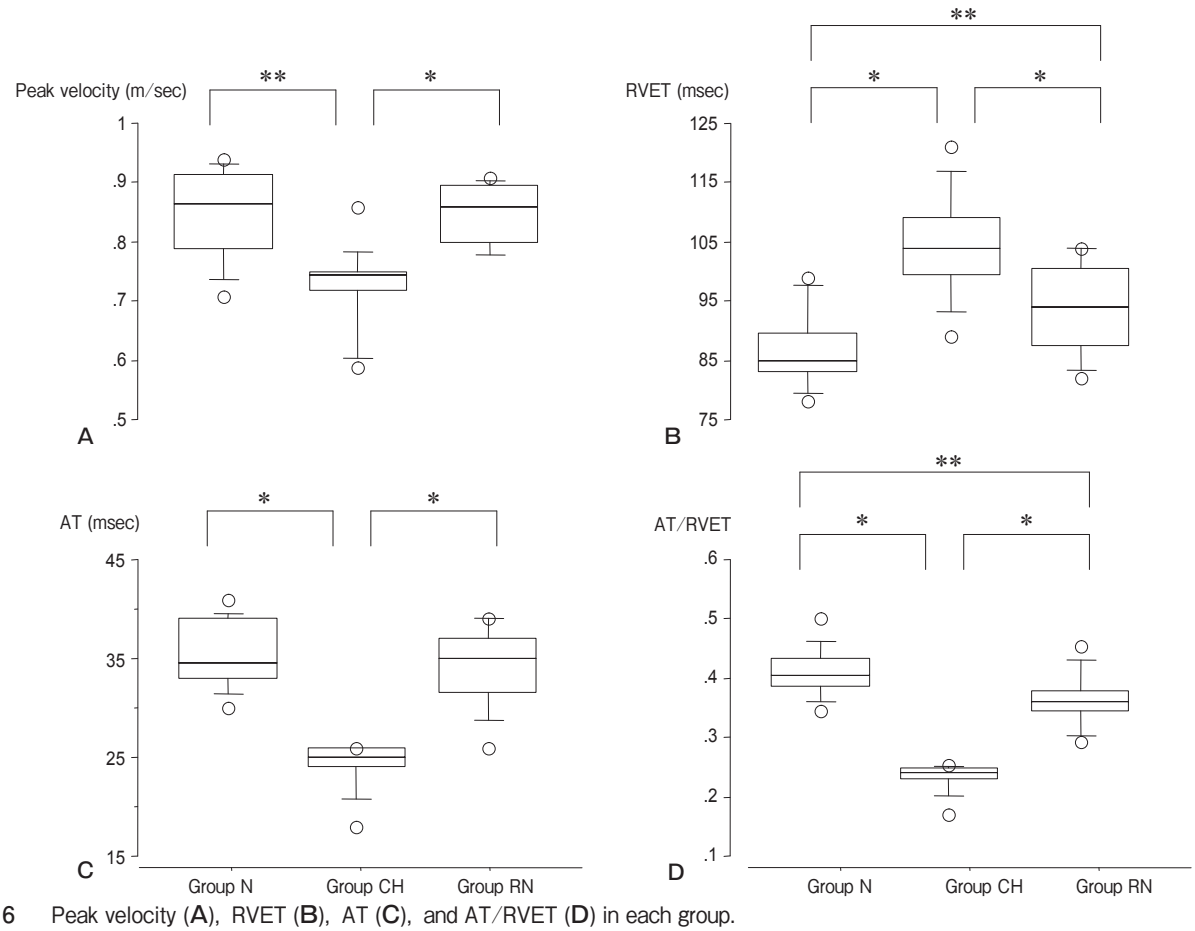

Fig. 6 Peak velocity (**A**), RVET (**B**), AT (**C**), and AT/RVET (**D**) in each group. The bar of each column in figure shows, from bottom to top, the 10th, 25th, 50th, 75th, and 90th percentile of each group. * and ** in figure indicate p values of <0.01 and <0.05 by the post-hoc test (Fisher's PLSD), respectively.

in relation to RV function, we analyzed echocardiographic parameters of LV and RV function after 8 weeks of hypoxia. However, further studies are needed to clarify the onset and progression of LV dysfunction in relation to RV function.

In our Doppler echocardiographic studies, we used xylazine to control heart rate as reported previously [15–19]. Such control might have a small impact on LV diastolic function. We could not clarify why there were some statistical differences in the parameters of LV systolic function. Larger FS and mVcf in the RN group compared with the other 2 groups might be a developmental change, while the frame rate of our system might be insufficient for the small heart of the rat, with limited resolution of the LV cavity and subsequent errors in measuring FAC.

Pressure data such as systemic or left ventricular end-diastolic pressure are commonly used to evaluate systolic or diastolic LV function. However, in our present model, it is technically impossible to measure either blood pressure in the hypoxic environment or left ventricular end-diastolic pressure without opening the chest.

Conclusion. In chronic hypoxic rats, although LV systolic function was preserved, diastolic function was impaired following LV distortion caused by PH and subsequent RV hypertrophy. In re-normoxic rats, however, the parameters of LV systolic and diastolic functions, pulmonary pressure and RV hypertrophy were similar to those of normoxic rats. Prolongation of RVET associated with PH, which acted as a phase-dependent factor, and RV hypertrophy and dilatation following RV pressure overload, which acted as a mechanical and anatomical factor, may have impaired

LV diastolic function through ventricular interaction.

Acknowledgments. The authors thank Tomomi Yoshinaka for her assistance with the echocardiography, and Dr. Peter M. Olley, Professor Emeritus of Pediatrics, University of Alberta, and Dr. Setsuko Olley for their kind assistance with the language of the paper.

References

1. Schena M, Clini E, Errera D and Quadri A: Echo-Doppler evaluation of left ventricular impairment in chronic cor pulmonale. Chest (1996) 109: 1446–1451.
2. Jorgensen K, Houlz E, Westfelt U, Nilsson F, Schersten H and Ricksten SE: Effects of lung volume reduction surgery on left ventricular diastolic filling and dimensions in patients with severe emphysema. Chest (2003) 124: 1863–1870.
3. Louie EK, Rich S and Brundage BH: Doppler echocardiographic assessment of impaired left ventricular filling in patients with right ventricular pressure overload due to primary pulmonary hypertension. J Am Coll Cardiol (1986) 8: 1298–1306.
4. Louie EK, Lin SS, Reynertson SI, Brundage BH, Levitsky S and Rich S: Pressure and volume loading of the right ventricle have opposite effects on left ventricular ejection fraction. Circulation (1995) 92: 819–824.
5. Stojnic BB, Brecker SJ, Xiao HB, Helmy SM, Mbaissouroum M and Gibson DG: Left ventricular filling characteristics in pulmonary hypertension: a new mode of ventricular interaction. Br Heart J (1992) 68: 16–20.
6. Xie GY, Lin CS, Preston HM, Taylor CG, Kearney K, Sapin PM and Smith MD: Assessment of left ventricular diastolic function after single lung transplantation in patients with severe pulmonary hypertension. Chest (1998) 114: 477–481.
7. Kim SH, Cho GY, Shin C, Lim HE, Kim YH, Song WH, Shim WJ and Ahn JC: Impact of obstructive sleep apnea on left ventricular diastolic function. Am J Cardiol (2008) 101: 1663–1668.
8. Dittrich HC, Chow LC and Nicod PH: Early improvement in left ventricular diastolic function after relief of chronic right ventricular pressure overload. Circulation (1989) 80: 823–830.
9. Mahmud E, Raisinghani A, Hassankhani A, Sadeghi HM, Strachan GM, Auger W, DeMaria AN and Blanchard DG: Correlation of left ventricular diastolic filing characteristics with right ventricular overload and pulmonary artery pressure in chronic thromboembolic pulmonary hypertension. J Am Coll Cardiol (2002) 41: 318–324.
10. Gurudevan SV, Malouf PJ, Auger WR, Waltman TJ, Madani M, Raisinghani AB, DeMaria AN and Blanchard DG: Abnormal left ventricular diastolic filling in chronic thromboembolic pulmonary hypertension. J Am Coll Cardiol (2007) 49: 1334–1339.
11. Aguglia G, Sgreccia A, Bernardo M, Carmenini E, Giusti De Marle, Reali A and Morelli S: Left ventricular diastolic function in systemic sclerosis. J Rheumatol (2001) 28: 1563–1567.
12. von Euler U, Liljestrand G: Observations on the pulmonary arterial blood pressure of the cat. Acta Physiol Scand (1946) 12: 301–320.
13. Morris-Thirgood J and Frenneaux M: Diastolic ventricular interaction and ventricular diastolic filling. Heart Fail Rev (2000) 5: 307–323.
14. Nakanishi K, Inoue M, Sugawara E and Sano S: Ischemic and reperfusion injury of cyanotic myocardium in chronic hypoxic rat model: Changes in cyanotic myocardial antioxidant system: J Thorac Cardiovasc Surg (1997) 114: 1088–1096.
15. Litwin SE, Katz SE, Morgan JP and Douglas PS: Serial echocardiographic assessment of left ventricular geometry and function after large myocardial infarction. Circulation (1994) 89: 345–354.
16. Litwin SE, Katz SE, Weinberg EO, Lorell BH, Aurigemma GP and Douglas PS: Serial echocardiographic-Doppler assessment of left ventricular geometry and function in rats with pressure-overload hypertrophy. Circulation (1995) 91: 2642–2654.
17. Masuyama T, Yamamoto K, Sakata Y, Doi R, Nishikawa N, Kondo H, Ono K, Kuzuya T, Sugawara M and Hori M: Evolving changes in Doppler mitral flow velocity pattern in rats with hypertensive hypertrophy. J Am Coll Cardiol (2000) 36: 2333–2338.
18. Shimizu N, Yoshiyama M, Takeuchi K, Hanatani A, Kim S, Omura T, Iwao H and Yoshikawa J: Doppler echocardiographic assessment and cardiac gene expression analysis of the left ventricle in myocardial infracted rats. Jpn Circ J (1998) 62: 436–442.
19. Jones JE, Mendes L, Rudd MA, Russo G, Loscalzo J and Zhang YY: Serial noninvasive assessment of progressive pulmonary hypertension in a rat model. Am J Physiol Heart Circ Physiol (2002) 283: H364–371.
20. Nootens M, Wolfkiel CJ, Chomka EV and Rith S: Understanding right and left ventricular systolic function and interactions at rest and with exercise in primary pulmonary hypertension. Am J Cardiol (1995) 75: 374–377.
21. Crystal GJ and Salem MR: Myocardial and systemic response to arterial hypoxemia during cardiac tamponade. Am J Physiol (1989) 257: H726–733.
22. Paridon SM, Bricker JT, Dreyer WJ, Reardon M, Smith EO, Porter CB, Michael L and Fisher DJ: The effect of hypoxemia on myocardial blood flow during exercise. Pediatr Res (1989) 25: 280–284.
23. Walley KR, Becker RC, Hogan RA, Teplinsky K and Wood LD: Progressive hypoxemia limits left ventricular oxygen consumption and contractility. Circ Res (1988) 63: 849–859.
24. Stritzke J, Mayer B, Lieb W, Luchner A, Doring A, Hense HW and Schunkert H: Haematocrit levels and left ventricular geometry: results of the MONICA Augsburg Echocardiographic Substudy. J Hypertens (2007) 25: 1301–1309.
25. Louie EK, Rich S, Levitsky S and Brundage BH: Doppler echocardiographic demonstration of the differential effects of right ventricular pressure and volume overload on left ventricular geometry and filling. J Am Coll Cardiol (1992) 19: 84–90.
26. Vonk-Noordegraaf A, Marcus JT, Holverda S, Roseboom B and Postmus PE: Early changes of cardiac structure and function in COPD patients with mild hypoxemia. Chest (2005) 127: 1898–1903.
27. Badke FR: Left ventricular dimensions and function during right ventricular pressure overload. Am J Physiol (1982) 242: H611–618.
28. Goto Y, Slinker BK and LeWinter MM: Nonhomogeneous left ventricular regional shortening during acute right ventricular pressure overload. Circ Res (1989) 65: 43–54.
29. Dohi K, Onishi K, Gorcsan J 3rd, Lopez-Candales A, Takamura T, Ota S, Yamada N and Ito M: Role of radial strain and displacement imaging to quantify wall motion dyssynchrony and chronic right ventricular pressure overload. Am J Cardiol (2008) 101: 1206–1212.